Another measure of the covalent/ionic nature of the complexes can be found in the gross atomic charge assigned to the metal and ligand, as shown in Table IV. This is equivalent to a Mulliken population analysis in the LCAO scheme. The pattern obtained here is different from that discussed previously considering only the f orbitals. Clearly, NpF_6 is the most covalent, but PaF_6^{2-} appears more covalent than UF_6^-. However, if the bonding is mainly ionic, then these results are consistent; i.e., the greater the charge on the complex as a whole the smaller the charge on the central ion. Since the F^- ion is the smallest and least polarizable halide ion, an overall charge on the complex will result in more charge being placed on the central metal ion. There appears to be little difference for the other halide ions.

Summary

This paper has described a systematic study of the 5f ligand field splitting in the $5f^1$ complexes $Pa^{IV}X_6^{2-}$, $U^VX_6^-$ (X = F, Cl, Br, I), and $Np^{VI}F_6$. A quasi-relativistic MS $X\alpha$ routine was used for this purpose. The trends observed in the f-orbital ligand field splitting appear to be principally ionic.

Contribution from the Department of Chemistry, University of Edinburgh, Edinburgh, EH9 3JJ Scotland, and the Inorganic Chemistry Department, University of Oxford, Oxford, OX1 3QR England

Electronic Structure of the Sulfur Nitrides. Ab Initio Calculations and Photoelectron Spectra

R. H. FINDLAY, M. H. PALMER,* A. J. DOWNS, R. G. EGDELL, and R. EVANS

Ab initio molecular orbital calculations of better than double-ζ quality are reported for SN, S_2N_2, S_4N_4, and a number of open-shell cationic states; midbond functions (on all molecules) and polarization functions on S_2N_2 are included. The gas-phase UV–photoelectron spectra (PES) up to 25 eV have been investigated and assigned on the basis of the calculations and cross-section changes under He I/He II irradiation. The electronic structures of S_2N_2 and S_4N_4 were investigated by transformation of the wave functions to a localized bond basis. A significant amount of S–S bonding was calculated for S_4N_4 but no N–N bonding. Across ring bonding was absent from S_2N_2.

Introduction

The long-known series of sulfur nitrides $(NS)_x$, where x = 1–4, have been widely investigated[1] and contrast sharply with the corresponding series $(NO)_x$ with x = 1, 2, 3, and 4 where only the first is well-known. Particular impetus to the study of the NS series has been provided by the remarkable electronic properties of the chain-type metallic conductor $(SN)_x$.[2]

Tetrasulfur tetranitride, S_4N_4 (**1**), is perhaps the most
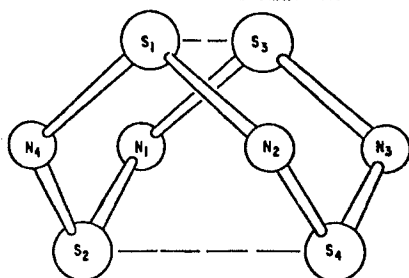
1

well-known member of the series, the molecular structures being based on a square-planar array of nitrogen atoms inserted within a approximately tetrahedral quartet of bridging sulfur atoms.[3] The dimer, disulfur dinitride S_2N_2 (**2**), consists
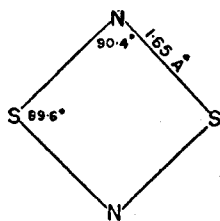
2

of alternating S and N atoms and is essentially square;[4] it is the usual precursor for polymeric $(SN)_x$.

In the present work we discuss the electronic structures of (a) S_2N_2 and (b) S_4N_4, both at their known crystal structure geometries,[3,4] and (c) SN, at the microwave geometry,[5] together with a number of open shell cationic states, for which the geometry is assumed to be the same as the ground state. The actual dimensions used were SN = 1.4957 Å, SN = 1.657 Å and SNS = 90.42° in S_2N_2, and SN = 1.616 Å and NSN = 104.5° in S_4N_4 (D_{2d}).

We assume that the molecular structures of the crystalline solids are still relevant to the gaseous S_2N_2 and S_4N_4 molecules; the similarity of the vibrational spectrum of S_2N_2 in the solid and gas phases supports this assumption. A number of previous electronic structure calculations have been reported for the present series of molecules: (a) for SN and/or SN^+ $X\alpha$[6] and ab initio (i) STO-3G,[7] (ii) extended basis,[8,9] and (iii) uhf;[10] (b) for S_2N_2 CNDO-2,[11,12] CNDO-S,[13] INDO (trip-

(1) Banister, A. J. *MTP Int. Rev. Sci.: Inorg. Chem., Ser. Two* **1975**, *3*, 41.
(2) Greene, R. L; Street, G. B. *Chem. Phys. One Dimensional Met. Proc. NATO Adv. Study Inst.* **1976**, 1. Geserich, H. P.; Pintschovius, L. *Festkorperprobleme*, **1976**, *16*, 65.
(3) Sharma, B. D.; Donohue, J. *Acta Crystallogr.* **1963**, *16*, 891.
(4) (a) MacDiarmid, A. G.; Mikulski, C. M; Russo, P. J.; Saran, M. S.; Garito, A. F.; Heeger, A. J. *J. Chem. Soc. Chem. Commun.* **1975**, 476. (b) Mikulski, C. M.; Russo, P. J.; Saran, M. S.; MacDiarmid, A. G.; Garito, A. F.; Heeger, A. J. *J. Am. Chem. Soc.* **1975**, *97*, 6358. (c) Cohen, M. J.; Garito, A. F.; Heeger, A. J.; MacDiarmid, A. G.; Mikulski, C. M.; Saran, M. S.; Kleppinger, J. *Ibid.* **1976**, *98*, 3844.
(5) Zeeman, P. B. *Can J. Phys.* **1951**, *29*, 174.
(6) Salahub, D. R.; Messmer, R. P. *J. Chem. Phys.* **1976**, *64*, 2039.
(7) Deutsch, P. W.; Curtiss, L. A. *Chem. Phys. Lett.* **1977**, *51*, 125.
(8) O'Hare, P. A. G. *J. Chem. Phys.* **1970**, *52*, 2992.
(9) Jafri, J. A.; Newton, M. D.; Pakkanen, T. A.; Whitten, J. L. *J. Chem. Phys.* **1977**, *66*, 5167.
(10) Török, F.; Pulay, P.; Szondy, T.; Nagy, P. *Acta Chim. Acad. Sci. Hung.* **1974**, *80*, 139.
(11) Adkins, R. R.; Turner, A. G. *J. Am. Chem. Soc.* **1978**, *100*, 1383. Adkins, R. R.; Dell, R.; Turner, A. G.; *J. Mol. Struct.* **1976**, *31*, 403.
(12) Kertesz, M.; Suhai, S.; Azman. A.; Kocjan, D.; Kiss, A. I. *Chem. Phys. Lett.* **1976**, *44*, 53.
(13) Salanek, W. R.; Lin, J. W-p.; Paton, A.; Duke, C. B.; Ceasar, G. P. *Phys. Rev. B.* **1976**, *13*, 4517.

*To whom correspondence should be addressed at the University of Edinburgh.
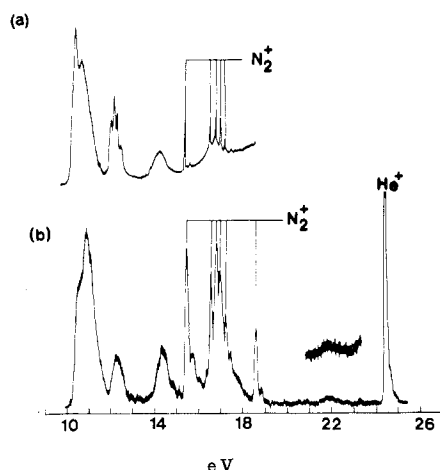
Figure 1. (a) He I and (b) He II PE spectra of S_2N_2.

let),[14] extended Hückel (EH),[12] Xα,[6] and ab initio (i) STO-3G,[7,12,15] (ii) extended basis,[9,15] and (iii) configuration interaction;[9] (c) for S_4N_4 CNDO-2,[16] CNDO-BW,[17] CNDO-S,[13] EH,[18,19] and Xα.[6] The present work is the first ab initio study with the same large basis sets for all three molecules such that the results can be compared. The gas-phase He I photoelectron spectrum (UPS) of S_2N_2[20] and S_4N_4 in the region 9–12 eV[13] have been confirmed and extended to the He II region; X-ray photoelectron spectra (XPS) have also been reported earlier for solid S_2N_2[21] and S_4N_4.[13]

Computational Methods

A linear combination of Gaussian orbital basis (LCGO) was used. Two main bases were used: (i) a medium-size minimum basis N (7s 3p), S (10s 6p 1d) scaled to optimize exponents in the NS bond as previously[22] and (ii) a new contraction[23] of the S (12s 9p) and N (9s 5p) bases by Dunning[24] and Veillard.[25] These final contractions are better than double ζ (with for example S [7s 2p]) and were further augmented for the individual compounds, the limiting factor being a program limitation to 126 basis functions. SN was augmented by an sp basis of midbond functions and $3d_S$, S_2N_2 by these plus an sp ring center and $3d_N$, and S_4N_4 by s-functions midbond (S–S and S–N). Thus the largest S_4N_4 calculation used 126 basis functions and generated 10 magnetic tapes of integrals (2400 ft/1600 bpi), and the SCF took 200 s/iteration on a CDC-7600; the largest bases for S_2N_2 and SN were 102 and 45, respectively. Total energies (all basis sets) and orbital energies (restricted to the valence shells of the molecules and including only selected calculations) are given in Tables I and II.

Experimental and Instrumental Methods

S_4N_4 was prepared by the reaction between ammonia and S_4N_3Cl suspended in CCl_4.[26,27] Following removal of the solvent in vacuo,
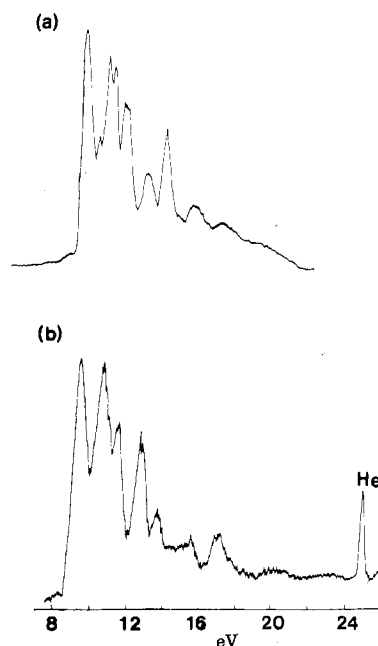
(14) Yamabe, T.; Tanaka, K.; Fukui, K.; Kato, H. *J. Phys. Chem.* **1977**, *81*, 727.
(15) Collins, M. P. S.; Duke B. J. *J. Chem. Soc., Chem. Commun.* **1976**, 701.
(16) Cassoux, P.; Labarre, J.-F.; Glemser, O.; Koch, W. *J. Mol. Struct.* **1972**, *13*, 405.
(17) Gopinathan, M. S.; Whitehead, M. A. *Can. J. Chem.* **1975**, *53*, 1343.
(18) Gleiter, R. *J. Chem. Soc. A* **1970**, 3174.
(19) Turner, A. G.; Mortimer, F. S. *Inorg. Chem.* **1966**, *5*, 906.
(20) Frost, D. C.; Le Geyt, M. R.; Paddock, N. L; Westwood, N. P. C. *J. Chem. Soc., Chem. Commun.* **1977**, 217.
(21) Sharma, J.; Downs, D. S.; Iqbal, Z.; Owens, F. J. *J. Chem. Phys.* **1977**, *67*, 3045.
(22) Palmer, M. H.; Findlay, R. H. *J. Chem. Soc., Perkin Trans. 2* **1974**, 1885; Palmer, M. H.; Gaskell, A. J.; Findlay, R. H.; Kennedy, S. M. F.; Nisbet, J. D. "Quantum Chemistry—The State of the Art, April 1974"; Saunders, V. R., Brown, J., Eds.; Science Research Council, London; 1975.
(23) Redshaw, M.; Palmer, M. H.; Findlay, R. H. *Z. Naturforsch. A* **1979**, *34*, 220.
(24) Dunning, T. *J. Chem. Phys.* **1970**, *53*, 2823.
(25) Veillard, A. *Theor. Chim. Acta* **1968** *12*, 405.
(26) Becke-Goehring, M.; Latscha, H. P. *Z. Anorg. Allg. Chem.* **1964**, *333*, 181.

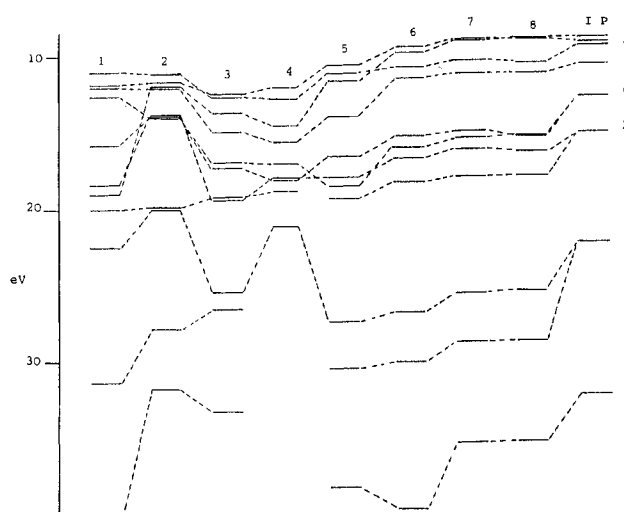**Figure 2.** (a) He I and (b) He II PE spectra of S_4N_4.

Figure 3. Orbital energies by symmetry and assignment for S_2N_2: (a) for semiempirical (1) CNDO-2, (2) CNDO-S, and (3) Xα; (b) for ab initio (4) Collins and Duke,[15] (5) minimal sp (present work), (6) minimal spd, (7) Jafri et al., and (8) largest basis (present work).

the crude product was recrystallized from benzene. The S_4N_3Cl was itself obtained by the method of Jolly et al.[28] This involves reaction between NH_4Cl and S_2Cl_2 to produce S_3N_2Cl, which was then allowed to interact with further S_2Cl_2 to yield the desired product.

S_2N_2 was generated by pyrolysis of S_4N_4 vapor over silver wool,[29] a process accomplished in a two-stage furnace attached to the volatile inlet probe of the spectrometer. The temperatures of the two furnace zones were adjusted to optimize counts from the product S_2N_2 without pronounced contamination of the spectrum by N_2.

PE spectra were measured on a Perkin-Elmer PS 16/18 spectrometer modified for He II measurements by the inclusion of a hollow-cathode discharge lamp and high-current power supply (Helectros Developments). Spectra were accumulated in a 512-channel multiscalar (Bentham Instruments Ltd.), analyzer voltages being swept by reference to a linear ramp produced by a D/A converter receiving channel address pulses from the scalar.

(27) Evans, R. unpublished work.
(28) Jolly, W. L; Maguire, K. D.; Rabinowitch, D. *Inorg. Chem.* **1963**, *2*, 1304.
(29) Becke-Goehring, M. *Inorg. Synth.* **1960**, *6*, 123.

Table I. Molecular Total Energies (au) for the Molecules as a Function of Basis Set

SN

	sp	spd	sp + midbond (sp)	spd + midbond (sp)
E_T	−451.833 59	−451.892 13	−451.905 14	−451.910 65
V/T	−1.999 16	−1.999 87	−2.000 24	−2.000 26

SN⁺

	double ζ			
	sp	spd	sp + midbond (sp)	spd + midbond (sp)
E_T	−451.484 79	−451.556 79	−451.574 26	−451.579 40
V/T	−2.000 07	−2.000 79	−2.001 19	−2.001 19

S_2N_2

	minimal spd	double ζ			
		sp	spd	spd + midbond + center	spd + midbond + center + pol
E_T	−902.023 02	−903.593 90	−903.785 96	−903.842 75	−903.859 92
V/T		−1.998 87	−1.999 99	−2.000 59	−2.000 42

S_4N_4

	minimal		double ζ	
	sp	spd	sp	sp + midbond
E_T	−1803.272 60	−1804.0827	−1807.140 78	−1807.384 09
V/T	1.960 1	−1.9622	−1.998 51	−1.999 52

Spectra were calibrated by reference to signals due to admixed nitrogen and helium ionizations.

PE spectra are shown in Figure 1 and 2, while ionization energy data are collected in Tables III and IV. The final correlations of the spectral and calculated data (using either Koopmans' theorem or open-shell calculations) are shown in Figures 3 and 4 and Tables I and II.

Principal Results and Spectral Assignments

SN. Shown in Tables I and II are results derived from the spin-restricted Hartree–Fock (RHF) calculations for the ground configuration $1\sigma^2 2\sigma^2 3\sigma^2 4\sigma^2 1\pi^4 5\sigma^2 6\sigma^2 7\sigma^2 2\pi^4 3\pi^1$, together with the results of unrestricted (UHF) calculations. The single occupancy of the 3π subshell leads to nondegeneracy of the 1π and 2π (π_x and π_y) levels in the lowest energy state. If these are constrained to be degenerate, the total energy is raised by ca. 0.013 au. The lowest RHF total energies we have calculated for SN and SN⁺ (Table I) are very similar to those of O'Hare (−451.932 86 and −451.574 63 au, respectively)[8] or Török et al.,[10] our values for the orbital energies follow the same symmetry sequence in energy for both the small and the largest calculations. For both NS and NS⁺ the energy lowering on addition of midbond sp functions is about the same as the addition of 3d to S (0.08 au). The nature of the lowering is however quite different in view of the different geometric positioning.

The dipole moment of SN, the only member of the present series to possess one, is very sensitive to basis set (cf. ref 8 also); addition of $3d_S$ and midbond functions leads to marked increases from the sp result (1.38 D) (which is near to that of Török et al.[10] at their best energy) to 1.75 D which is close both to that of O'Hare (1.73 D) and to the experimental spectral value of 1.86 D;[30] it is interesting to note that O'Hare's wave function for SN appears to have more d functions on N than S, contrary to normal practice.

The full photoelectron spectrum of SN has not yet been reported, but a recent UV–PES value for the first IP is 8.87 eV,[31] to be compared with an earlier value of 9.85 eV[8] on the
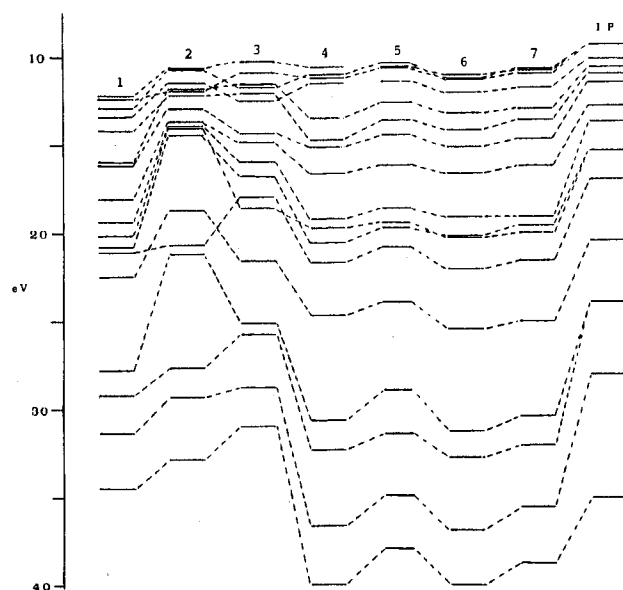

Figure 4. Orbital energies by symmetry and assignments for S_4N_4: (a) for semiempirical (1) extended Hückel, (2) CNDO-S, and (3) Xα; (b) for ab initio (present work) (4) minimal sp, (5) minimal spd, (6) double ζ sp, and (7) double ζ sp + midbond (S/S, S–N).

basis of electron-impact data. The present minimal basis set calculations yield 11.09 and 9.75 eV by using Koopman's theorem and the ΔSCF (IP = $E_{ION} − E_{MOL}$) procedure, respectively. The largest present double-ζ bases yield much better numerical agreement, 11.16 and 9.01 eV, respectively; the values from O'Hare[8] are 10.10 and 9.75 eV, respectively, Török et al.[10] gave 9.81 and 9.00 eV, while the CNDO-S[13] and Xα[16] methods yield 5.48 and 8.3 eV (Koopmans' theorem only), respectively.

When an unrestricted Hartree–Fock calculation was performed for the SN radical, with the largest basis set, the total energy was lowered to −451.926 83 au. The first IP then

(30) Amano, T.; Saito, S.; Hirota, E. *J. Mol. Spectrosc.* **1969**, *32*, 97. Carrington, A.; Howard, B. J.; Levy, D. H.; Robertson, J. C. *Mol. Phys.* **1968**, *15*, 187. Revision in: Byfleet, C. R.; Carrington, A.; Russell, D. K. *Ibid.* **1971**, *20*, 271.

(31) Dyke, J. M.; Morris, A.; Trickle, I. R. *J. Chem. Soc., Faraday Trans. 2* **1977**, *73*, 147.

Table II. Valence-Shell Orbital Energies (eV) for SN, S_2N_2, and S_4N_4 (Selected Basis Sets)

SN

	minimal spd	double ζ spd + midbond (largest)
3π	11.78	11.16
2π	12.78/13.68	12.63/13.55
7σ	13.74	14.55
6σ	19.86	20.82
5σ	33.44	34.25

S_2N_2

	minimal spd	double ζ spd + $3d_S + 3d_N$ + midbond + center
$2b_{3g}$	11.25	10.59
$1b_{2g}$	10.34	10.62
$4b_{3u}$	10.95	12.21
$5b_{2u}$	13.61	12.87
$7a_g$	16.31	16.93
$2b_{1u}$	18.21	16.96
$2b_{1g}$	17.67	18.03
$6a_g$	19.00	19.59
$4b_{2u}$	27.06	27.18
$3b_{3u}$	30.20	30.45
$5a_g$	38.00	37.09

S_4N_4

	minimal spd	double ζ spd	double ζ sp + midbond
$3a_2$	10.47	11.21	10.63
$8b_2$	10.49	10.97	10.71
$9a_1$	10.27	11.29	10.93
$4b_1$	11.38	11.95	11.72
$7b_2$	12.57	13.18	12.87
$11e$	13.51	14.09	13.49
$10e$	14.35	15.04	14.60
$9e$	16.06	16.51	16.12
$8a_1$	18.56	19.02	18.53
$6b_2$	19.62	20.20	19.56
$2a_2$	19.35	20.13	19.94
$7a_1$	20.78	22.02	21.55
$8e$	23.85	25.43	24.94
$5b_2$	28.87	31.21	30.32
$3b_1$	31.33	32.66	32.02
$7e$	34.87	36.80	35.75
$6a_1$	37.82	39.92	38.66

Table III. Ionization Energy Data (eV) and Assignments for S_2N_2

IP	assignt	IP	assignt
10.51	$2b_{3g}$	14.42	$7a_g, 2b_{1u}$
10.81	$1b_{2g}$	16.77[a]	$2b_{1g}, 6a_g$
11.06 (sh)	$4b_{3u}$	22.02[b]	$4b_{1u}, 3b_{3u}$
(12.17)		~32[c]	$5a_g$
12.28[d]	$5b_{2u}$		
(12.39)			
(12.51)			

[a] Value quoted by Frost et al.[20] [b] He II. [c] Estimate from XPS data.[21] [d] Vertical.

Table IV. Ionization Energy Data (eV) and Assignments for S_4N_4

| IP	assign	IP	assign
9.36	$3a_2, 8b_2, 9a_1$	15.27	$6b_2, 2a_2$
10.11	$4b_1$	16.93	$7a_1$
10.60	$7b_2$	20.4[a]	$8e$
10.92	$11e$	23.9[a]	$5b_2, 3b_1$
11.44	$10e$	~28[b]	$7e$
12.74	$9e$	~31 (35)[b]	$6a_1$
13.66	$8a_1$		

[a] He II. [b] Estimate from XPS data.[13]

stable with respect to change of basis set. This is even more true if the semiempirical calculations[6,11-13] are compared. The present work set out to extend the range of total energy to see whether such a stability in order could be found. Our smallest basis set (minimal spd) yielded an order only different from the largest Jafri et al.[9] set by a single interchange of orbitals. In the largest present basis a further change from the Jafri order was obtained, leading to the order (increasing binding energy) $2b_{3g}$ (π_S) < $1b_{2g}$ (π_N) < $4b_{3u}$ (LP_N) < $5b_{2u}$ (LP_S) < $7a_g$ (LP_N/LP_S) < $2b_{1u}$ (π). The magnitude of these shifts relative to our other large bases or the Jafri et al. order[9] is small, and we regard the largest set as (effectively) having the Hartree–Fock limiting values. The relevance of these conclusions and the open-shell calculations to the photoelectron system is described below. First we discuss the UV–PE spectral appearance for S_2N_2 with change of irradiation energy and then the comparison with earlier work.

The He I photoelectron spectrum of S_2N_2 obtained in the present work (Figure 1a) was in substantial agreement with that reported by Frost et al.[20] although we were unable to obtain a spectrum entirely free of N_2. This made it difficult to examine further the poorly resolved fine structure near 16 and 18 eV observed by Frost et al.

The He II spectrum of S_2N_2 (Figure 1b) revealed an additional weak band at 22-eV binding energy. Noticeable differences in appearance between the He I and He II spectra, after allowance for the larger slit width in the latter, were (a) a marked enhancement of the intensity of the fourth band relative to the third band (taking into account analyzer transmission differences) and (b) an obvious decline in the intensity of the first band at 10.5 eV relative to the second at 10.8 eV under He II conditions. The first difference is discussed below, while the 10.5/10.8 eV change is consistent with a relatively high $3p_S$ component in the 10.5-eV band and more $2p_N$ in the 10.8-eV band. This is supported by known cross-section differences for S and N.[32]

Because of the substantial overlay between the He I and He II photoelectron spectra in our instrument, it is not usually practicable to observe IP's beyond 25 eV; thus bands associated with MO's of dominant N_{2s} character are not located. A maximum of 5 out of the 11 valence-shell bands are accessible to us. The XPS spectrum of solid S_2N_2 (at -100 °C) under Mg $K\alpha$ conditions shows groups of ionization maxima at 4.2, 7.0, 9.8, 15.8, and 25 eV[21] to high binding energy of the "instrument zero level". The highest binding energy peak must contain the N_{2s} levels, while the the four lower binding energy levels must be associated with the centroids of the groups of IP's in the UV–PES; these centroids are at 11.2, 14.4, 16.8, and 22 eV, yielding a linear shift between the two instrument scales of ca. 7 eV; this corresponds to the resultant of the Fermi level, charging effects, and work function. Thus the N_{2s} levels of S_2N_2 must lie near 32 eV in the gas phase; this is consistent with gas phase XPS data on N_2 where the N_{2s} levels are at 25.0 (σ_u) and 37.3 eV (σ_g), giving a mean value of 31 eV,[33]

became 9.72 eV (Koopmans' theorem) and 9.45 eV (ΔSCF). The dipole moment was slightly lower at 1.67 D (cf. 1.75 D). The virial ratio V/T was -1.99989 and $\langle S^2 \rangle$ 0.774; both are close to the Hartree–Fock values -2.00000 and 0.750, respectively.

S_2N_2. The total energy, arising from the largest basis set calculation used here on S_2N_2, is the lowest yet reported (previous -903.7901 au[9]) for a single configuration study and comparatively close to the recent CI study by Jafri et al.[9] which yielded -903.91387 au for the ground state. A survey of the earlier ab initio results[7,9,12,15] shows that the orbital energy levels in *sequence* by symmetry representation are far from

(32) Schweig, A.; Thiel, W. *J. Electron Spectrosc.* **1974**, *3*, 27; *J. Chem. Phys.* **1974**, *60*, 951.

while pyrrole has N_{2s} at 29.5 eV $(4a_1)$[34] etc. We thus have six main bands in which to identify 11 energy levels. The first band shows clear evidence of 3 IP's. Intensity patterns in the He II spectra suggest that the third and fourth PE bands (near 14 and 17 eV) also relate to more than one ionization process. These are assigned to two IP's in each case, yielding a final series of groupings (low to high binding energy) 3:1:2:2:2:1. This correlation is shown in Figure 3, together with energy levels calculated by various methods; the general level of sophistication of the calculations rises from left to right, and slight trends in orbital energy for a particular symmetry type have been utilized in the derivation of the final correlation. The experimental spectrum (Figure 1) shows four main IP's, and these can be correlated with groups of orbital energies (A, B, C, D; see Figure 3) from all calculations. The CNDO-2[11] and CNDO-S[13] groupings do not appear to fit with the experimental intensity ratios above; the $X\alpha$ calculations[6] are more satisfactory but do not separate groups A and B well; an arbitrary 6 eV has been added to these orbital energies to bring them near to the experimental range. The small ab initio basis sets[7,15] do not yield satisfactory A and B groupings. This is rectified in all of the present calculations and in those of Jafri et al.[9] None of the Koopmans' theorem studies yields an internal 3:1 ratio in group A, and in the largest basis-set calculations this arises from the LP_N level $(4b_{3u})$ being placed at too high a binding energy. Direct calculation of the first three ionization potentials for the largest basis set yields $(E_{ION} - E_{MOL})$ 9.33 $(2b_{3g})$, 9.97 $(1b_{2g})$, and 10.63 eV $(4b_{3u})$, that is, three equally spaced IP's, a result which is consistent with the broad envelope observed. Finally, we note the marked fine structure on the IP at 12.3 eV; this is calculated to be from $5b_{2u}$ (LP_S). We have noted that lone-pair sulfur levels in several heterocyclic compounds often show fine structure and contrast with the corresponding LP_N; an example is 1,2,5-thiadiazole (3) which shows well-defined structure on the LP_S

3
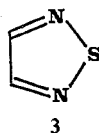
level assigned to the IP at 13.39 eV.[35] Overall, the assignment of the spectrum according to the large basis set of the present work seems satisfactory. Of the earlier methods only the $X\alpha$ calculations[6] are of comparable utility.

S_4N_4. The He I spectrum (Figure 2) is in good agreement with that of Salanek et al.[13] whose spectral range was only 9–12 eV but contains four extra bands to higher energy; a further two IP's were observed under He II irradiation. Comparison of the latter spectrum with the solid-state X-ray photoemission spectrum of Salanek et al.[13] indicates that the bands at 20.4 and 23.9 eV (He II) correspond to maximma on the XPS profile at ca. 13- and 17-eV binding energy. This again leads to a scale shift of ca. 7 eV between the Fermi level and the UV–PES data. Thus the remaining inner-valence-shell ionizations are at ca. 28- and 35-eV (or possibly 31-eV) binding energy; the 35-eV choice seems more likely by comparison with S_2N_2 and on a correlation of the calculated and experimental data below. These last two IP's lie beyond our observable range. We thus have a total of 13 distinct IP's in the PE spectra. Of the 22 orbitals in the valence shell 10 orbitals form

degenerate pairs, and so 17 distinct ionizations are anticipated. Comparison of the experimental IP's with the canonical MO energies shows that the assignment is not trivial.

A correlation, by symmetry, of the extended Hückel,[18,19] CNDO-S,[13] $X\alpha$,[6] and present ab initio calculations and a final correlation with the observed photoelectron spectrum are shown in Figure 4, with selected data in Table II. The orbital energies of the $X\alpha$[6] calculation were arbitrarily increased by 4 eV to bring them to the correct range. The orbital ordering of the EH and CNDO-S calculations is similar except for two marked changes of sequence of individual MO's. Neither of these two calculations leads to reasonable groupings of MO's or to the sequence of IP's of gradually extending separation on moving to higher binding energy. This criterion is roughly fulfilled by the $X\alpha$[6] and present ab initio calculations; there are however marked changes in order of orbitals in the low-binding-energy sets, and the latter calculations seem more consistent with the experimental envelope. Furthermore, the ab initio results seem to settle toward particular groups as the number of basis functions is increased.

Further useful guidance on the assignment was obtained from a comparison of the He II and He I intensity patterns and from changes in calculated orbital energy with basis set (below). We find (a) a marked decrease in intensity of the band at 13.7 eV on switching to He II excitation and (b) minor changes in the band profile near 10.9 eV. Earlier experimental and theoretical studies indicate that the S_{3p} one-electron ionization cross section is markedly lower than that for N_{2p} under He II irradiation.[32] Detailed examination of the wave functions shows that extensive delocalization and mixing of N and S character occur in most orbitals. Notable exceptions are the two sulfur lone-pair orbitals (LP_S) $8a_1$ and $7b_2$. The former $(S_1 + S_2 + S_3 + S_4)$ is almost pure sp hybrid, while the latter $(S_1 - S_2 + S_3 - S_4)$ is almost pure S_{3p} in character. Similarly the two orbitals $9a_1$ and $4b_1$ are of dominant nitrogen lone-pair character (LP_N). Detailed population analyses are shown in the Tables V and IV. We expect therefore that intensities in the low-energy region of the He II spectra will largely reflect the number of distinct orbitals associated with each PE band, except that the structure related to the $8a_1$ and $7b_2$ levels should be anomalously weak. Finally we note the changes of calculated orbital energy with refinement of the basis set (Figure 4). The group of 4 orbital energies near 11 eV in the sp-basis-set calculation with 56 functions clearly splits 3:1 in the larger basis calculations (126). Slight respacing of the next group of 4 levels occurs. The two levels near 20 eV become nearly degenerate in the largest calculations. Finally open-shell calculations in the largest basis for the first three IP's $(=E_{ION} - E_{MOL})$ yield the values 10.22 $(^2B_2)$, 10.39 $(^2A_2)$, and 10.84 eV $(^2A_1)$, confirming the closeness of these ionizations. With these considerations in mind we arrive at the assignment shown in Figure 4 and Table III. Particular support is then provided by (a) the marked diminution in intensity of the well-resolved IP at 13.7 eV with the switch from He I to He II excitation, a change consistent with the assignement to S_{LP} $(8a_1)$ and (b) the change in groupings of IP's with basis set to $9a_1$, $3a_2$, $8b_2$ (corresponding to the first band) and $4b_1$, $7b_2$, $11e$ (corresponding to the second group IP's).

Discussion

Molecular Energy Levels. Several features of the electronic structure of S_2N_2 warrant discussion. With use of the above assignments, the splittings of symmetric and antisymmetric lone-pair combinations are 5.5 eV for $LP_N^{\pm}$ and 4.5 eV for $LP_S^{\pm}$; in both cases the "normal" order LP_X^- is to lower binding energy (X = S, N). Both these values are extremely large and in part arise from the close geometric arrangement of atoms in planar S_2N_2. The structure has few direct

(33) Siegbahn, K.; Nordling, C.; Johansson, G.; Hedman, J.; Heden, P. F.; Hamrin, K.; Gelius, U.; Bergmark, T.; Werme, L. O.; Manne, R.; Baer, Y. "ESCA Applied to Free Molecules," North-Holland Publishing Co.: Amsterdam, 1969; p 64.

(34) Gelius, U.; Allan, C. J.; Johansson, G.; Siegbahn, H.; Allison, D. A.; Siegbahn, K. *Phys. Scr.* **1971**, *3*, 237.

(35) Heilbronner, E. In "Physical Methods in Heterocyclic Chemistry"; Katritzky, A. R., Ed. Academic Press: London, 1974; Vol. IV, p 1.

Table V. Mulliken Population Analyses for SN, S_2N_2, and S_4N_4

SN

	largest basis uhf	
	S	N
1s + 2s + 3s	5.7778	3.8306
$2p_\sigma + 3p_\sigma$	2.6921	1.2631
$2p_\pi + 3p_\pi$	6.7552	1.9735
$3d_S$	0.0679	...
midbond s	0.4447	
$\quad\quad p_\sigma$	−0.0360	
$\quad\quad p_\pi$	0.2311	
total	15.6129	7.3871

S_2N_2

	largest basis	
	S	N
1s + 2s + 3s	5.7369	3.7326
$2p_\sigma + 3p_\sigma$	5.6729	2.3470
$2p_\pi + 3p_\pi$	3.4984	1.3139
$3d_S/3d_N$	0.1348	0.0200
midbond s	0.2092	
$\quad\quad p_\sigma$	0.0131	
$\quad\quad p_\pi$	0.0619	
center s	0.0369	
$\quad\quad p_\sigma$	−0.1069	
$\quad\quad p_\pi$	0.0201	
total[a]	15.3148	7.6852
overlap pop.		
S-N	0.3461	
S-S	−0.2471	
N-N	−0.1257	

S_4N_4

	double ζ		minimal spd	
	S	N	S	N
1s + 2s + 3s	5.7821	3.6379	5.6970	3.6066
$(2p + 3p)_{total}$	9.0127	3.8054	9.5294	3.8481
$2d_S$	...	...	0.3188	0
midbond S-S	0.0412		...	...
midbond S-N	0.3604		...	...
total[a]	15.1964	7.8036	15.5453	7.4547
overlap pop.	0.4135		0.3913	
S-N	0.3465		0.1248	
S-S	−0.0997		−0.0251	
N-N				

[a] Total populations include one-half of each midbond term for all bonded atoms; in S_2N_2 one-fourth of the center term is added to each atom.

analogies, but it is worth noting that the corresponding value for the $LP_N^{\pm}$ splittings in pyrazine (**4**) is 1.72 eV; there the

4
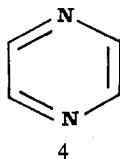
binding-energy order is reversed ($a_g < b_{2u}$), and this can be interpreted in terms of either "through-bond" coupling[35] or perturbation by nitrogen[36] of the benzenoid e_{2g} level. 1,4-Dithiane (**5**), which is of course nonplanar, has a similarly
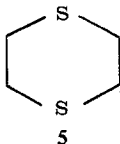

5

(36) Palmer, M. H.; Gaskell, A. J.; Findlay, R. H. *J. Chem. Soc., Perkin Trans. 2* **1974**, 778.

Table VI

Mulliken Analysis for S_2N_2 with Midbond and Center sp Functions

	S			N		midbond		center	
	%s	%p	%d	%s	%p	%s	%p	%s	%p
$2b_{3g}$	0	96	0	0	0	0	4	0	0
$1b_{2g}$	0	0	3	0	90	0	7	0	0
$4b_{3u}$	0	8	1	8	77	6	1	0	−1
$5b_{2u}$	9	58	1	0	26	8	0	0	−2
$7a_g$	6	22	0	17	47	1	7	−1	0
$2b_{1u}$	0	52	1	0	39	0	7	0	2
$2b_{1g}$	0	42	2	0	47	8	1	0	0
$6a_g$	52	20	0	24	4	0	0	0	0
$4b_{2u}$	80	−1	1	0	14	10	−1	0	−3
$3b_{3u}$	0	12	2	77	1	12	−3	0	−1
$5a_g$	29	5	1	44	8	13	0	1	0

Mulliken Analysis for S_4N_4 on the Basis of Double-ζ Calculations

	S		N			S		N	
orbital	3s	3p	2s	2p	orbital	3s	3p	2s	2p
$8b_2$	4	20	0	76	$2a_2$	0	47	0	53
$3a_2$	0	1	0	99	$6b_2$	4	53	0	43
$9a_1$	5	55	12	27	$7a_1$	31	40	29	0
$4b_1$	0	8	7	85	$8e$	42	17	20	21
$7b_2$	1	93	0	6	$5b_2$	89	0	0	11
$11e$	5	34	2	59	$3b_1$	0	13	85	2
$10e$	4	27	14	55	$7e$	31	6	56	7
$9e$	8	50	3	39	$6a_1$	39	8	44	9
$8a_1$	22	60	1	17					

rationalized,[35] but much smaller, splitting for LP_S of 0.45 eV.[37] Finally we draw attention to the near degeneracy (ΔE = ca. 0.5 eV) of the two upper π levels in S_2N_2 ($1b_{2g}$ and $2b_{3g}$) and the large separation (6 eV) from the inner π level ($2b_{1u}$). This is reminiscent of the Hückel description of the π-isoelectronic valency shell of the cyclobuta-1,3-diene dianion (**6**). The latter

6

has a degenerate (e″) subshell at $E = 0$ and a further π level (a_2'') at $E = 2\beta$. The $1b_{2g}$ and $2b_{3g}$ MO's of S_2N_2 are notable for the extreme degree of localization of the electron density on N and S, respectively.

The D_{2d} arrangement of S atoms in S_4N_4 yields LP_S combinations of a_1, e, and b_2 symmetry. Our interpretation and calculations indicate the prevalence of the "natural" binding-energy (BE) order for the through-space interactions, namely, $b_2 < e < a_1$. The close proximity of the S_4 arrangement in S_4N_4 to a tetrahedron is accompanied by the small separation of the e and b_2 levels ($\Delta E = 0.5$ eV from the IP's), which would be degenerate (t) if T_d symmetry prevailed.

The two S_4N_4 LP_N levels $9a_1$ and $4b_1$ mentioned above occur in the unexpected BE order $9a_1 < 4b_1$ ($\Delta E = 0.75$ eV). This is comprehensible only in terms of limited mixing of the symmetric LP_N and LP_S group orbitals; the out-of-phase combination $LP_N - LP_S$ is largely of N_{2p} character (85%) while the the in-phase combination $LP_N + LP_S$ is of mixed S_{3p} (55%) and N_{2p} (27%) character (Table VI).

Direct comparison of S_2N_2 with S_4N_4 is of limited value owing to the very different geometric characteristics of the two compounds. The LP_N levels at 10.8 (π) and 11.05 eV (σ) in S_2N_2 are close to the σ values 9.36 (a_1) and 10.92 eV (b_1) in S_4N_4; however, more marked differences are evident for LP_S with values of 12.3 (b_{2u} in S_2N_2) and 10.6 eV (b_2 in S_4N_4), while the symmetric combination $LP_N + LP_S$ is at 16.8 eV

(37) Sweigart, D. A.; Turner, D. W. *J. Am. Chem. Soc.* **1972**, *94*, 5599. Bock, H.; Wagner, G. *Angew. Chem., Int. Ed. Engl.* **1972**, *11*, 150.

($7a_g$) in S_2N_2 and 13.7 eV ($8a_1$) in S_4N_4. Clearly the smaller ring size allows a more extensive interaction in S_2N_2; however, the classical representation of both molecules has the fragment $-N-S-N-$, and the lower binding energies deduced for the LP_S levels in S_4N_4 could derive in part from a weakening of the S–N linkage accompanied by S–S bonding, the change in electronegatively of the attached groups then being important. This is relevant to the localized MO study below.

Few compounds possess structures analogous to S_4N_4, and it is difficult therefore to compare our IP's with those for other molecules. One species containing a pseudotetrahedral array of sulfur atoms is the twist form of the tetramethyltetrathiane (7). The LP_S levels for this molecule have been reported to

7
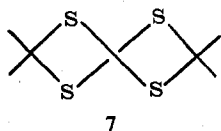
lie in the range 8.23–9.44 eV,[38] significantly lower than in S_4N_4; no doubt this is partially a result of "replacement" of the highly electronegative N by Me_2C. The sulfur cage molecules As_4S_3 and P_4S_3 have lower IP's than those found in the present study, namely, for As_4S_3 8.86 (a_1) and 9.31 eV (e) and for P_4S_3 9.24 (a_1) and 9.57 eV (e).[39] However, a clear identification of the nature of these IP's is awaited; if they originate in LP_S, electronegativity differences are apparent, as well as an inversion of the expected order. The leading bands at IP's of 9.4–10.19 eV in the UV–PES of S_8 (D_{4d} symmetry[40] probably relate to differing nodal properties for this molecule; ab initio studies[41] suggest the order $3a_1 \approx 3e_3 < 3e_1 \approx 3e_2$ for the orbitals of lowest binding energy, at variance with the Xα–SW results.[40]

Mulliken Analyses. The analysis of S_2N_2 and S_4N_4, each for a single basis set, is given in Tables V and VI; the one chosen for S_2N_2 is the largest used except that the $3d_N$ polarization functions are absent, while the midbond (MB) and ring center (C) functions are included. The S_2N_2 data show that the MB and C functions are utilized only to a small percentage in the occupied MO's. As a consequence the S_4N_4 data refer to the sp double-ζ basis only. Direct comparison of the present results for S_2N_2 and S_4N_4 with those from the Xα calculations[6] is not easy since the analysis of the latter calculations records only the atomic s/p ratios for S and N rather than percentages of the total; thus it is not possible for most MO's to tell whether the S/N ratio of populations is similar to those of the present work. The internal s/p ratios are comparatively similar for both S_2N_2 and S_4N_4 with the exception that the Xα calculations seem to lead to much higher proportions of S_{3s} in the levels at high binding energy. (It should be noted that the orbital numbering system in ref 6 refers to valence shell orbitals only.) A more direct comparison of the present wave functions for S_4N_4 is with the CNDO-S results of Salanek et al.[13] Except in those cases where the S/N proportions are controlled by symmetry, and hence in agreement, the present data (Table VI) are markedly different for most MO's. Furthermore, direct comparison of the individual MO compositions and the corresponding orbital energies shows that a change of ordering occurs within the three "e" orbitals in the center of the valence shell (9e–11e here, 3e–5e in ref 13). These extensive differences, confirmed by the schematic diagrams,[13] are somewhat surprising, since it is usually thought that the density function varies comparatively little with the

method of calculating the wave function in high-symmetry molecules; i.e., a degree of topological control is usually thought to occur in the wave function.

Total population analyses for SN, S_2N_2, and S_4N_4 show a consistent pattern of behavior for a particular basis set, and the overall effect is donation of electron density for sulfur to nitrogen. In the cases of SN and S_2N_2 both σ- and π-donation mechanisms occur; a σ/π separation is not possible with S_4N_4. The $3d_S$ orbitals appear to play a comparatively minor role although, as is usual, their inclusion has the effect of reducing the bond polarities. The polarization $N^{\delta-}-S^{\delta+}$ is predicted to be similar in S_4N_4 and S_2N_2 and much larger than in SN itself. The values of the midbond function populations are always substantially larger than the $3d_S$ or $3d_N$ components when these are added to the basis. Thus for SN^+ the total (s + p) midbond population is 0.885 e, of which almost half is the s function and the remainder largely π_x/π_y: the p_σ component is actually negative (–0.08 e). The net effect of these orbitals is to concentrate electron density in the central-bonding region rather than disperse it (negative populations). This is the reverse of the influence of atomic-centered $3d_S$ or $3d_N$ functions. The midbond functions play a rather smaller role in S_2N_2 on a proportionate basis of four SN bonds; none-the-less the total (1.58 e) is large. By contrast, the center functions are much less important in S_2N_2. The π components of all the midbond and center terms are much smaller than the σ functions. The center s function here is significantly negative (–0.13 e), thus reducing the electron density at the ring center and dispersing it back to the internuclear axes. When midbond S–N and S–S functions were inserted separately and then jointly into the double-ζ S_4N_4 calculation, the resultant contributions were much larger in the S–N (0.36 e) than S–S bonds (0.08 e). As a test of variational as opposed to bonding effects, functions were placed near nitrogen but remote from the attached S atoms; these yielded a population of 0.06 e, i.e., similar to those of the S–S midpoint functions. The mechanism of the S–S terms thus could be purely variational. However, an alternative possibility is that they are important only in the presence of polar S–N bonds.

The possibility of cross-ring and cross-cage bonding is of course a matter of particular interest. The overlap populations for S_2N_2 (Table V) clearly show that, while adjacent atoms are bonded (positive overlap), cross-ring bonding is absent, presumably as a result of the strong interactions between the opposing lone-pair electrons. The position for S_4N_4 is somewhat different; here positive overlap populations are found for adjacent pairs of S atoms, albeit significantly smaller than those for adjacent pairs of S and N atoms.

Localized Orbitals for S_4N_4 and S_2N_2. Further insight into the bonding of these two molecules was obtained by transformation of the canonical wave function to a localized orbital basis (LMO) by using the Foster–Boys method[42] which maximizes the sum of the squares of the distance between orbital centroids.

For S_4N_4, four types of localized orbital emerge from the transformation, viz., S–N bonds (×8), S–S bonds (×2), LP_S (×4), and LP_N (x8). The degree of localization, showing the extent of two center Table VII character, is high except for the LP_N orbitals; in these the remaining density is distributed among the four now nonequivalent S atoms, the major component being associated with the cis S atom, i.e. that closest to the LP_N.

In keeping with earlier semiempirical studies,[17] we find that the centroid (C) of the S–S bond orbital lies above the S–S

(38) Guimon, M. F.; Guimon, C.; Metras, F.; Pfister-Guillouzo, G. *J. Am. Chem. Soc.* **1976**, *98*, 2078.
(39) Cannington, P. H.; Whitfield, H. J. *J. Electron Spectrosc.* **1977**, *10*, 35.
(40) Richardson, N. V.; Weinberger, P. *J. Electron Spectrosc.* **1975**, *6*, 109.
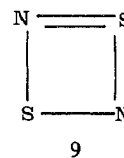(41) Findlay, R. H. unpublished results.

(42) Foster, J. M.; Boys, S. F. *Rev. Mod. Phys.* **1960**, *32*, 300. Boys, S. F. In "Quantum Theory of Atoms, Molecules and the Solid State"; Lowdin, P. O., Ed.; Academic Press: New York, 1966. Newton, M. D.; Switkes, E. *J. Chem. Phys.* **1971**, *54*, 3179.

Table VII. Localized MO's for S_4N_4 and S_2N_2:
Minimal spd Results

S_4N_4

| | % localizn | S | | | N | |
		3s	3p	3d	2s	2p
S–N (×8)	97.98	26.6	69.9	3.5	12.9	87.2
S–S (×2)	92.03	15.1	83.9	1.0	0	0
LP$_S$ (×4)	97.64	54.6	45.3	0.1	0	0
LP$_N$ (×8)	84.0	0	0	0	41.1	58.9

S_2N_2

| | % localizn | S | | | N | |
		3s	3p	3d	2s	2p
S–N (×4)	97.8	21.3	74.8	3.9	26.0	74.0
S–N (×2)	96.5	11.7	85.2	3.1	15.4	84.6
LP$_S(\sigma)_A$	98.5	64.5	35.5	0	0	0
LP$_S(\sigma)_B$	98.3	62.5	37.5	0	0	0
LP$_S(\pi)_A$	92.9	0	99.6	0.4	0	0

axis but (in our hands) by only 0.06 Å, corresponding to an angle SCS of 2.6°.

Overall, therefore, and in agreement with the findings of ref 16, 17, and 19, we conclude that the molecule best fits the Lewis structure (**8**). The population analyses also show the

8

tendency towards S^+–N^- character required by the classical structure (**8**).

The valence-shell LMO's of S_2N_2 show a number of characteristics in common with the features deduced from semiempirical studies,[11] although in the present work σ and π MP's were allowed to mix, thus leading to "bent" bonds rather than pure σ or π LMO's.[11] The final LMO wave function corresponds to the structure (**9**), i.e., a single canonical form based on the pair resonance hybrids that can be drawn for a combination of S^{II} and S^{IV} bonding. The initial canonical

9

wave function is of course symmetrical, and the present form clearly shows the equivalence of the two S^{II} and S^{IV} centers. A consequence of this is that the two σ LP$_S$ are not strictly identical since a σ/π separation has occurred at one side of the molecule and not at the other. The low level of delocalization of π LP$_S$ is reminiscent of the CNDO-2 wave function.[11,12] The absence of cross-ring bonding, as noted above from the negative overlap populations, is also confirmed.

Concluding Remarks

The earlier work on the photoelectron spectra of S_2N_2 and S_4N_4 has been extended by the measurement of the He II spectra. Detailed interpretation of the data for S_4N_4 is difficult, but the new He II measurements, in conjunction with XPS data and the ab initio calculations by using more than one basis set, lead to a plausible interpretation for the complete valence-shell spectrum. This assignment differs significantly from that advanced on the basis of earlier semiempirical calculations. In contrast, the spectrum of S_2N_2 is relatively straightforward in assignment. The present results are in substantial agreement with those of earlier work, except that the first IP is assigned to a π_S rather than a π_N level.
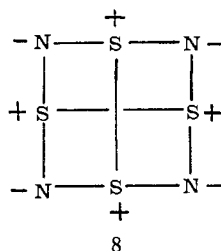
A general feature emerging from the calculations, and consistent with the experimental photoelectron spectra, is that interactions among "lone-pair" orbitals are important in the sulfur nitrides. In the case of S_2N_2 these lead to a very large "through-space" splitting of LP$_S^\pm$ and LP$_N^\pm$ levels. The situation in S_4N_4 is more complicated, but the unexpected occurrence of the totally symmetric LP$_N$ level as one of the most weakly bound orbitals is best interpreted in terms of through-space interactions between symmetric LP$_S$ and LP$_N$ group orbitals.

The conversion of our wave functions to a localized basis shows the absence of cross-ring N–N bonding and the presence of significant S–S bonding between each of the pairs of adjacent sulfur atoms in S_4N_4. By contrast, there is no cross-ring bonding in S_2N_2.

Contribution from the Inorganic Chemistry Laboratory, Oxford, OX1 3QR, Great Britain,
and the Department of Chemistry, University of Edinburgh, Edinburgh, EH9 3JJ, Great Britain

Electronic Structure of the Group 5 Oxides: Photoelectron Spectra and ab Initio Molecular Orbital Calculations

RUSSELL G. EGDELL,* M. H. PALMER, and R. H. FINDLAY

Gas phase He I and He II photoelectron spectra of the group 5 oxides P_4O_6, As_4O_6, Sb_4O_6, and P_4O_{10} are reported. Qualitative descriptions of the electronic structure of these molecules are discussed with reference to ab initio molecular orbital calculations for the species P_4, P_4O_6, and P_4O_{10}. On the basis of the experimental and theoretical results, correlations among electronic energy levels within the series (i) P_4, P_4O_6, and P_4O_{10} and (ii) P_4O_6, As_4O_6, and Sb_4O_6 are suggested.

Introduction

The group 5 oxides are introduced in many chemistry textbooks as prototype examples of cage inorganic structures.[1]

Recent interest in cage and cluster compounds has been stimulated by the belief that they may serve as molecular "models" for solid-state systems.[2]

---

* To whom correspondence should be addressed at the Inorganic Chemistry Laboratory, Oxford.

(1) E.g.: Huheey, J. E. "Inorganic Chemistry"; Harper and Row: London, 1975.
(2) E.g.: Muetterties, E. L. *Science* **1977**, *196*, 4292.